ACADEMIC PRESS

Journal of Solid State Chemistry 169 (2002) 160–167

JOURNAL OF SOLID STATE CHEMISTRY

www.academicpress.com

Large cavities with nanosized channels in a three-dimensional neutral framework: structure and properties of a novel oxovanadium arsenate: $As_2V^{IV}V^{V}O_{26}(OH)] \cdot 8H_2O$

Yongnan Zhao,[a,*] Yafeng Li,[b] Qingsheng Liu,[b] Xiangming Chen,[b] Yong Wang,[b] Xiuhong Li,[b] Ming Li,[b] and Zhenhong Mai[b]

[a] *Center for Condensed Matter Physics and Institute of Physics, Chinese Academy of Sciences, P.O. Box 603-79, Beijing 100080, People's Republic of China*

[b] *Department of Chemistry, Jilin University, Changchun 130023, China*

Received 3 April 2002; received in revised form 26 August 2002; accepted 12 September 2002

Abstract

A novel open-framework oxovanadium arsenate has been hydrothermally synthesized. It crystallizes in space group $I\bar{4}3m$ with cell parameters of $a = 16.708(2)$ Å, $V = 4664.4(9)$ Å^3 and $Z = 4$. Its structure is composed of a new type of decavandium cluster, which is constructed by two pentamers. Linking this decavanadate by AsO_4 tetrahedral, a three-dimensional open-framework structure forms, which possesses large cavities. These high symmetric cavities interconnected through 12-membered ring windows forming a three-dimensional channel system. Catalytic measurements indicate that this compound is active for phenol hydroxylation using hydrogen peroxide as the oxidant. Catechol, hydroquinone and benzoquinone are the main products with 15.8% conversion of phenol (taking no account of the secondary product of tar) and 59.6% selectivity for hydroquinone, when the reaction was performed in water at 60°C for 6 h.

Keywords: Hydrothermal synthesis; Oxovanadium arsenate; Single crystal structure; Open-framework; Catalytic property

1. Introduction

Controlled linking of simple building blocks to create multifunctional structures, which contain cavities and display specific properties, is a key reaction in the biological and material science. The best example is the chemistry of host–guest interactions, which spans the entire range from three- and two-dimensional to one- and zero-dimensional discrete host structures (supramolecular inorganic structures) [1–3]. As a branch of host–guest compounds, open-framework materials are of great interest from both the industrial and academic point of view due to their catalytic, adsorbent, and ion-exchange properties [4–6]. Hydrothermal syntheses have been proved to be an exiting and promising method to prepare new and structurally complex, hybrid, organic–inorganic, solid-state compounds and have led to the dramatic expanding of the field of open-framework inorganic materials during the last decades. While the large voids, chemical stability and size discriminatory sorptive behavior of zeolites have rendered them very useful, open-framework solids containing transition elements could provide novel properties including catalytic, photochemical and magnetic properties, inaccessible in the main group system [7]. Following the successful introduction of transition metals into the zeolite AlPOs and GaPOs and the discovery of open-framework solids with coordination numbers larger than four [8,9], the syntheses of phosphates containing transition elements have been widely studied. Transition metals with different valence and coordination numbers give more possibilities to prepare materials with larger dimensionalities or unique framework topologies or novel polyhedral connectivities. Oxide examples include zinc, ion and beryllium phosphates and arsenates [10]. The contemporary interest in oxovanadium phosphates reflects not only their practical applications as catalysts,

*Corresponding author. Fax: +10-8264-9531.
E-mail address: zhaoyn@263.net (Y. Zhao).

0022-4596/02/$ - see front matter
PII: S0022-4596(02)00039-7

ionic conductivity, ion-exchanger, versatile intercalation properties and magnetic properties but also their fundamental chemistry, which is characterized by unusual structural complexity [11]. Vanadium in different valence states (V, IV, III) can form tetrahedral, square pyramidal and octahedral coordination and aggregate by condensation of polyhedron through shared oxygen atoms. Template-controlled linking of these units has led to a large number of oxovanadium phosphates with open-framework structures [12–18], in which two eye-catching results are $[(CH_3)_2NH_2]K_4[V_{10}O_{10}(H_2O)_2(OH)_4(PO_4)_7]\cdot 4H_2O$ [19], which containing chiral double helices consisting of interpenetrating spirals confirms that inorganic species can also mimic biologically relevant structures, and the three-dimensional frameworks of $[HN(CH_2CH_2)_3NH]K_{1.35}[V_5O_9(PO_4)_2]\cdot xH_2O$ and $Cs_3[V_5O_9(PO_4)_2]\cdot xH_2O$ providing the largest cavities and the lowest framework densities known up to now [20]. Besides these three compounds, an interesting structure is the mixed-valence materials, which exhibits large elliptical channels (7×18 Å) [21]. Our recent interests are the pursuit of oxovanadium borophosphates and boroarsenates. And two exciting compounds, which are constructed by 12-membered ring crown-shaped clusters, have been synthesized [22,23]. In order to prepare oxovanadium boroarsenate, a novel three-dimensional oxovanadium arsenate $[As_2V_8^{IV}V_2^{V}O_{26}(H_2O)]\cdot 8H_2O$, denoted VAs-1, was synthesized. Here we report its synthesis, single crystal structure and catalytic properties.

2. Experimental section

2.1. Synthesis and initial characterization

Vanadium oxide (V_2O_5, 99%), KH_2AsO_4 (99%), triethylenetetraamine (TETA, >95%), HCl (35%) and boric acid (H_3BO_3, 99.5%) are used as the starting materials. All reagents are used without further purification.

The oxovanadium arsenate VAs-1 was synthesized under mild hydrothermal conditions starting from a mixture of V_2O_5, KH_2AsO_4, H_3BO_3 and TETA. Typically, 0.4 g V_2O_5, 0.5 g KH_2AsO_4, 0.5 g H_3BO_3, 0.5 mL TETA, 1.2 mL HCl were dispersed in 20 mL water. The starting mixture was vigorously stirred to attain homogeneity. The final solution was transferred into a 40 mL Teflon-lined autoclave and crystallized at 160°C for 2 days. The initial pH value of the mixture was 8.0. The reaction led to the formation of dark-green cubic crystal in ca. 40% yield (based on vanadium) without apparent variation of the pH value. This crystal was washed with water, dried at room temperature and used for further characterizations.

Powder X-ray diffraction (XRD) patterns were performed on a Riguku D/MAX-III diffractometer with Ni-filtered Cu$K\alpha$ radiation. The record speed was 8°C min^{-1} over the range of 4–40°C at room temperature. Comparison of the experimental and simulated XRD patterns shows that the compound obtained was a monophasic product. Thermogravimetric analysis (TGA, Perkin-Elmer TGA-7 thermgravimetric analyzer) shows that the weight loss occurs in three steps between 30°C and 700°C. The total loss of 31.6% corresponds to the loss of water [13.5% from 30°C to 220°C (calcd. 13.1%)] and the collapse of the framework. VAs-1 is thermally unstable and transforms into an amorphous phase after heating at 200°C for 2 h. Chemical analysis was carried out on a Perkin-Elmer 240C elemental analyzer with the vanadium to arsenic ratio of 4.9. Infrared spectra were collected on a Nicolet Impact 410 FT IR spectrometer in the range of 400–4000 cm^{-1} using the KBr disk method. A large number of bands observed in the region of 400–1300 cm^{-1} are assigned to be the As–O and V–O vibrations. Additional strong absorption bands at 3000–3500 cm^{-1} are contributed to the O–H bending and stretching vibrations of the water molecules.

Catalytic properties were measured in phenol hydroxylation system using H_2O_2 (30%) as the oxidant. Hydroxylation was performed in a round-bottom flask equipped with a magnetic stirrer, a reflux condenser and a thermostat. The reaction system consisted of 50 mg catalyst and 10 mL solvent with the phenol to hydrogen peroxide ratio of 1. The product distribution analyses were recorded by gas chromatography (Shimadzu GC-14B) with a fused silica capillary column (code: CBP1-M50-025). The initial programmed temperature was 120°C. Temperature was increased in 4°C min^{-1} at the first stage and 8°C min^{-1} at the second stage. The final temperature was 200°C. The calculations of phenol conversion and the product yield were based on the amount of phenol added. The secondary product of tar, which was difficult quantified by GC, was not accounted for in the conversion calculation.

2.2. Structure determination

A single crystal of VAs-1 with approximate dimensions of $0.1\times 0.1\times 0.1$ mm^3 was selected and mounted on a glass fiber. Crystal structure determination was carried out on a Siemens P4 four circle diffractometer at 293(2) K. The unit cell was obtained and refined by 27 well-centered reflections in the range of $5.73^\circ<\theta<12.29^\circ$. Data were collected in the range of $1.72^\circ<\theta<25.06^\circ$. Of the total of 2915 reflections collected, 633 were independent with 440 observed. Raw intensities were corrected for Lorentz and polarization effects, and for absorption by empirical method based on ψ-scan data. Although V(1) and V(3), as well as O(1) and O(3), appear to be related by a mirror plane

Table 1
Crystal data and structure refinement for VAs-1

Empirical formula	$H_{18}As_2O_{35}V_{10}$
Formula weight	1237.38
Temperature	293(2) K
Wavelength	0.71073 Å
Crystal system, space group	Cubic, $I\bar{4}3m$
Unit cell dimensions	$a = 16.708(2)$ Å
Volume	4664.4(9) Å^3
Z, Calculated density	4, 1.762 g cm^{-3}
Absorption coefficient	3.395 mm^{-1}
$F(000)$	2376
Crystal size	$0.1 \times 0.1 \times 0.1$ mm^3
Theta range for data collection	1.72–25.06°
Limiting indices	$-1<h<9$, $-1<k<18$, $-18<l<18$
Reflections collected/unique	2915/633 [$R_{int} = 0.0486$]
Absorption correction	Semi-empirical
Max. and min. transmission	0.9333 and 0.8130
Refinement method	Full-matrix least squares on F^2
Data/restraints/parameters	633/0/71
R indices [$I > 2\sigma(I)$]	$R_1 = 0.0569$, w$R_2 = 0.0775$
R indices (all data)	$R_1 = 0.1099$, w$R_2 = 0.1392$

Table 2
Atomic coordinates ($\times 10^4$) and equivalent isotropic displacement parameters (A$^2 \times 10^3$) for 1. U_{eq} is defined as one third of the trace of the orthogonalized U_{ij} tensor

	x	y	z	U_{eq}
As	5000	0	2500	17(2)
V(1)	3875(5)	768(6)	3875(5)	20(4)
V(2)	5000	1473(9)	5000	22(4)
V(3)	6125(8)	715(6)	3875(8)	23(7)
O(1)	3444(8)	1522(8)	3444(9)	29(6)
O(2)	5000	2443(10)	5000	35(8)
O(3)	6705(12)	1322(12)	3295(13)	30(8)
O(4)	4171(9)	43(12)	3064(9)	21(4)
O(5)	6077(10)	1097(15)	4903(10)	41(8)
O(6)	5000	0	5000	106(7)
OW1	7343(12)	2657(12)	4757(11)	175(11)
OW2	7583(13)	2417(13)	3450(13)	66(13)

Table 3
Bond lengths [Å] and angles [deg] for 1

	Bond	Lengths (Å)	
As–O(4)#1	1.676(6)	As–O(4)#2	1.676(6)
As–O(4)	1.676(6)	As–O(4)#3	1.676(6)
V(1)–O(1)	1.620(5)	V(1)–O(4)#4	1.884(6)
V(1)–O(4)	1.884(6)	V(1)–O(5)#5	2.116(6)
V(1)–O(5) #5	2.116(6)	V(2)–O(5)	1.913(9)
V(2)–O(2)	1.600(8)	V(2)–O(5)#5	1.913(9)
V(2)–O(5)#4	1.913(9)	V(2)–O(5) #5	1.913(9)
V(3)–O(4)#6	1.921(9)	V(3)–O(3)	1.706(9)
V(3)–O(5)	1.834(9)	V(3)–O(5)#5	1.834(9)
V(3)–O(4)#3	1.921(9)		
	Bond	Angle (deg)	
O(4)#1–As–O(4)#2	110.6(5)	O(4)#1–As–O(4)	108.9(5)
O(4)#2–As–O(4)	108.9(5)	O(4)#1–As–O(4)#3	108.9(5)
O(4)#2–As–O(4)#3	108.9(5)	O(4)–As–O(4)#3	110.6(5)
O(1)–V(1)–O(4)#4	109.1(6)	O(1)–V(1)–O(4)	109.1(6)
O(4)#4–V(1)–O(4)	87.2(7)	O(1)–V(1)–O(5)#5	100.6(8)
O(4)#4–V(1)–O(5)#5	150.3(7)	O(4)–V(1)–O(5)#5	85.9(9)
O(1)–V(1)–O(5)#5	100.5(6)	O(4)#4–V(1)–O(5)#5	85.9(10)
O(4)–V(1)–O(5)#5	150.3(7)	O(5)#5–V(1)–O(5)#5	85.9(7)
O(2)–V(2)–O(5)#5	106.4(9)	O(2)–V(2)–O(5)#5	106.4(9)
O(5)#5–V(2)–O(5)#5	96.6(10)	O(2)–V(2)–O(5)#4	106.4(9)
O(5)#5–V(2)–O(5)#4	74.1(8)	O(5)#5–V(2)–O(5)#4	147.2(8)
O(2)–V(2)–O(5)	106.4(9)	O(5)#5–V(2)–O(5)	147.2(8)
O(5)#5–V(2)–O(5)	74.1(7)	O(5)#4–V(2)–O(5)	96.6(10)
O(5)–V(3)–O(4)#6	89.0(11)	O(3)–V(3)–O(5)	105.0(10)
O(3)–V(3)–O(5)#5	105.0(10)	O(5)–V(3)–O(5)#5	79.3(11)
O(3)–V(3)–O(4)#3	103.9(8)	O(5)–V(3)–O(4)#3	150.7(7)
O(5)#5–V(3)–O(4)#3	89.0(11)	O(3)–V(3)–O(4)#6	103.9(8)
O(5)#5–V(3)–O(4)#6	150.8(7)	O(4)#3–V(3)–O(4)#6	88.5(6)
V(2)–O(5)–V(1)#5	88.7(5)	V(3)#3–O(4)–V(1)	82.1(7)
V(3)–O(5)–V(2)	103.0(11)	V(3)–O(5)–V(1)#5	142.1(5)
As–O(4)–V(3)#3	128.5(6)	As–O(4)–V(1)	129.5(5)

Symmetry transformations used to generate equivalent atoms: #1: $-y+1/2$, $x-1/2$, $-z+1/2$; #2: $y+1/2$, $-x+1/2$, $-z+1/2$; #3: $-x+1$, $-y$, z; #4: z, y, x; #5: $-z+1$, y, $-x+1$; #6: $-z+1$, $-y$, x.

at $x = 0$, attempts to refine the structure in space group $Im3m$ were failed. The structure was solved by direct methods using SHELXTL (ver.5.01) software package. The final peaks larger than 1 are adjacent to the metal atoms. The final full-matrix least-squares refinement on F^2 afforded residuals $R1 = 0.0569$ and w$R2 = 0.0775$ for observed reflections [$I \geqslant 2\sigma(I)$]. Crystallographic details are given in Table 1. The atomic positional and displacement parameters are listed in Table 2. The bond lengths and bond angles are given in Table 3.

3. Results and discussions

3.1. Synthesis

Hydrothermal synthesis has been proved to be a promising and mild method to prepare metastable open-framework structures with or without inorganic or organic cations as templates. The dark-green cubic crystal of VAs-1 was hydrothermally obtained from the reaction of V_2O_5: 1.25 KH_2AsO_4: 3.8 H_3BO_3: 1.5 TETA: 5.5 HCl: 500 H_2O at 160°C for 2 days. The organoamine, HCl and boric acid are absolute requirement for isolation of VAs-1, although both the single crystal refinement and the chemical analysis indicate that there is no organic, boron and chlorine species in VAs-1. According to the literature [16], the V(IV) species that predominates in aqueous solution at low pH value is $VO(H_2O)_5^{2+}$. As the pH increases, hydrolysis and condensation lead to the soluble $VO(OH)(H_2O)_4^{+}$ and $(VO)_2(OH)_2(H_2O)_6^{2+}$. The role of organoamine appears to be adjustment of the pH value and maintenance of the reducing reaction environment. These provide the vanadium in the soluble V(IV) state. Using ethylenediamine replaced the triethylentetraamine, VAs-1 can also be synthesized with poor crystallinity. Although a large

number of open-framework materials have been hydrothermally synthesized, the role of one or several reactants is not understood, such as $FeCl_3 \cdot 6H_2O$ in the synthesis of (VOBOPO-1) [24] and phenylphosphonic acid and Et_2NH in the synthesis of $[HN(CH_2CH_2)_3NH]K_{1.35}[V_5O_9(PO_4)_2] \cdot xH_2O$ [20]. In the case of VAs-1, the role of HCl and boric acid is unknown. Attempts to prepare VAs-1 without organoamine, HCl and H_3BO_3 were failed.

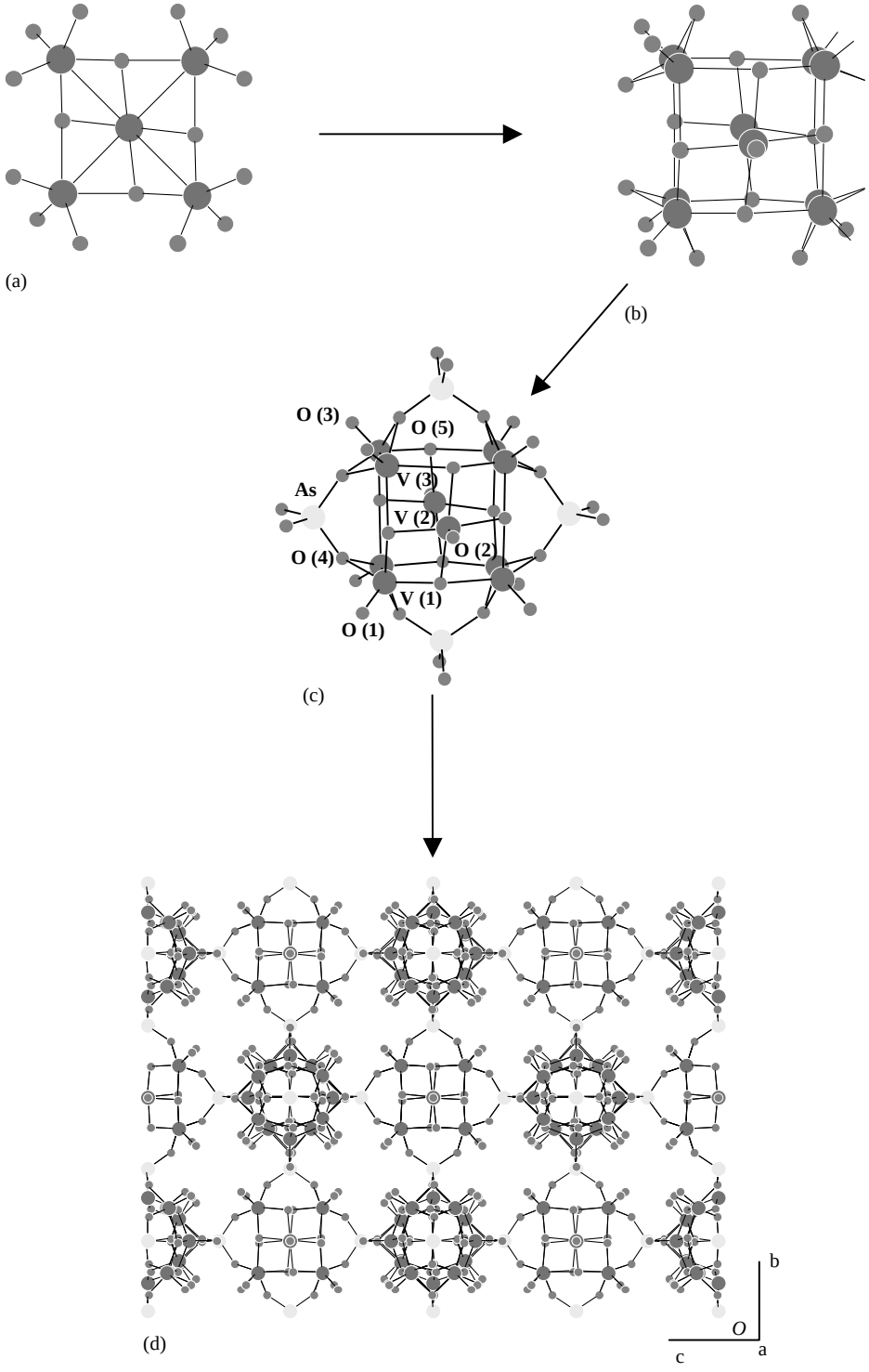

Fig. 1. Schematic representation of the formation of the three-dimensional structure of VAs-1. Formation of VAs-1 can be viewed as undergoing the following processes: (a) pentavanadium motif; (b) decavandium cluster cage; (c) the decavandium cluster capped with AsO_4 tetrahedral; (d) two adjacent perpendicular decavanadium cluster connected by AsO_4 tetrahedral forming the three-dimensional architecture.

3.2. Structural description

Structure refinement indicates that VAs-1 crystallized in the space group $I\bar{4}3m$. The asymmetric unit of VAs-1 contains one As, three V atoms and eight oxygen atoms, of which three oxygen atoms belong to the guests (Fig. 1c). The crystallographically distinct As atom, having the geometry observed for monoarsenate, shares four oxygen atoms with the adjacent vanadium atoms with all As–O distances of 1.662(6) Å. All vanadium atoms exist in square pyramidal coordination. The V(2) atom is coordinated by a terminal oxo group O(2) and four μ_3-oxygen atoms O(5). The geometry around each vanadium V(1) or V(3) atoms is linked by four μ_3-oxygen atoms O(4) and O(5) and an apical terminal vanadyl V=O(1) group. The five adjacent vanadium atoms form an unusual cross-shaped V_5 pentamer with a central V(2) atom sharing each of its four basal edges with four additional square-pyramidal vanadium atoms. Two pentamers fused oppositely forming a decavanadium cage with a water molecule encapsulated in the center (Fig. 1b). The V(2)−O(6) distance is 2.46 Å. The decavanadium cluster provides the fundamental structural motif for the structure of VAs-1. The decanuclear cage $[V_8^{IV}V_2^{V}O_{27}]$ of VAs-1 shows four $[V_4O_{16}]$ windows with four AsO_4 tetrahedral capped forming a closed cage (Fig. 1c). The AsO_4 tetrahedral connects two perpendicular decavanadium clusters by four μ_3-oxygen atoms. Hence, a three-dimensional network forms (Fig. 1d). The framework can be viewed as constructed through the following steps: (I) the VO_5 square pyramidal are joint together to form the pentamer; (II) two pentamers fused positively to form the decavanadium cluster with an encapsulated water molecule; (III) the AsO_4 groups cap the decavanadium clusters and link two adjacent perpendicular decavanadium clusters to form cavities and the channel system (Fig. 1). According to the bond valence sum calculation and charge balance requirement [25], VAs-1 is formulated as $[As_2V_8^{IV}V_2^{V}O_{26}(H_2O)]\cdot 8H_2O$. The assignment of oxidation states for vanadium atoms are confirmed by the valence sum calculation results for V1, V2, V3 of 4.05, 5.06 and 4.16. The valence calculation identifies O(6) [BVS = 0.27] as a water molecule. The prominent feature of VAs-1 is the large voids in the V–As–O framework centered at (000), which have rigorous $\bar{4}3m$ symmetry with diameter of 18.42 Å (Fig. 2a). These cavities are highly symmetric and filled with eight water molecules.

The V_5 pentamer of VAs-1 is closely related to the $[V_5O_9(PhPO_3)_{4/2}]$ unit of the molecular clusters $[\{NH_4Cl\}_2V_{14}O_{22}(OH)_4(PhPO_3)_8]^{6-}$ [26], the core structure of the $[V_5O_9(\text{thiophene-2-carboxylate})_4]^{2-}$ [27] and the block unit of $[HN(CH_2CH_2)_3NH]K_{1.35}[V_5O_9(PO_4)_2]\cdot xH_2O$ and $Cs_3[V_5O_9(PO_4)_2]\cdot xH_2O$ [20], which possess the lowest framework densities and the largest cavities observed in the open-framework materials. The pentamer clusters has been reported to play a pronounced bending with V–V–V angles subtended at the apex of approximately $125\pm10^\circ$ [20]. The combination of this curvature, the distance between the AsO_4 groups and the relatively low charge per volume of the pentamer, all favor metrically large structures that would be difficult to fill all space in dense fashion. The large volume of the cavities is reflected in the low framework metal atom density. There are only about 10.3 metal (As, V) atoms per 1000 $Å^3$. Compared with 12.7 and 11.1 atoms per 1000 $Å^3$ for faujasite and cloverite, respectively [28], VAs-1 belongs to those of the lowest framework densities among the known open-framework compounds. This cavity possesses 24-membered ring at the maximum diameter viewed along the cross-section (Fig. 2a) perpendicular to any one of the [111] directions. The interconnection of the large cavities

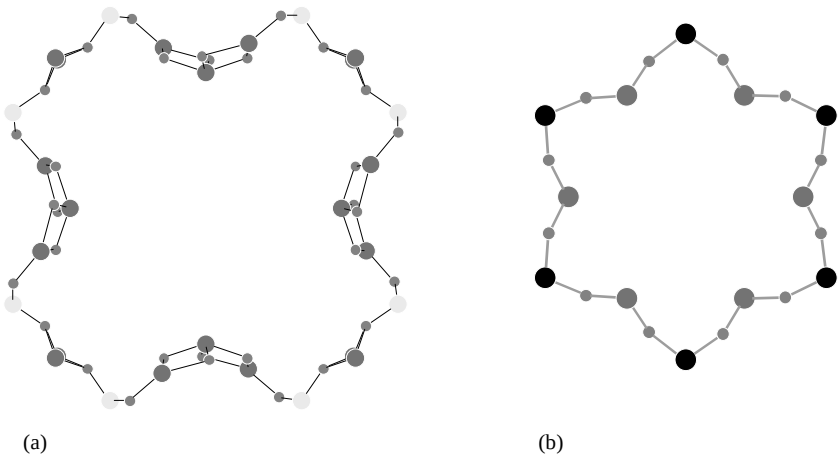

(a) (b)

Fig. 2. The cross-sectional view, perpendicular to any one of the [111] directions, of the 24-ring central section (a) and the hexagonal 12-ring window of the cavity in VAs-1.

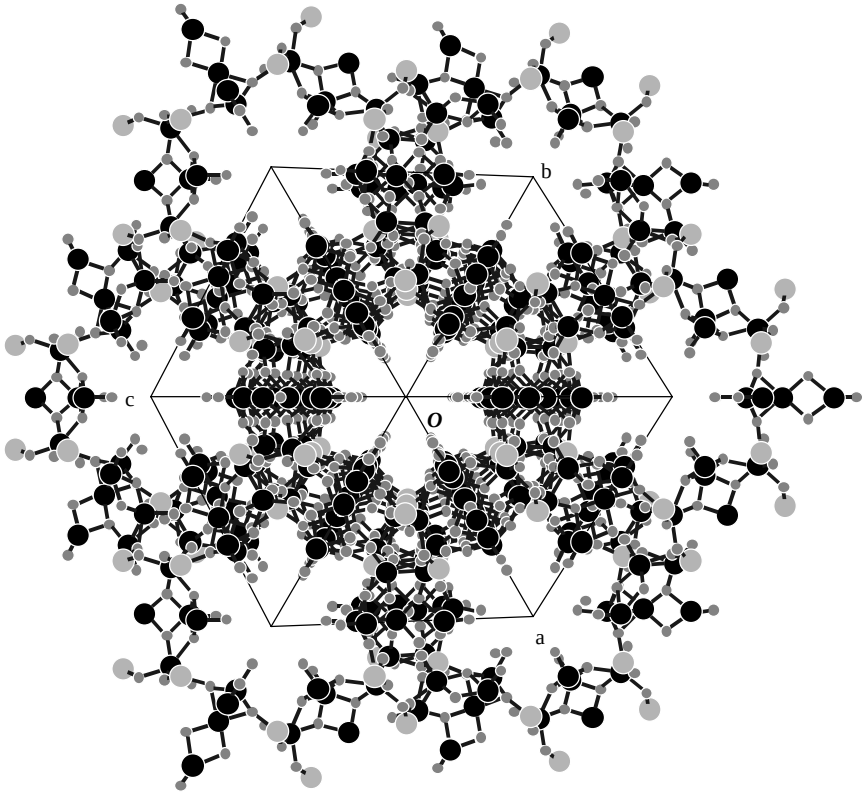

Fig. 3. Structure of VAs-1 viewed along the [111] direction showing the 12-membered channels.

gives rise to fascinating channel architecture. Each cavity has six hexagonal 12-membered ring windows of 11.99 Å in diameter that surround the origin in an octahedral fashion (Fig. 2b). Through these windows, the cavity communicates with six neighboring symmetrical equivalent cavities along (111) directions. These channels intersect at the cavities forming a three-dimensional channel system (Fig. 3).

It is well-known that polyoxovanadates have a profound tendency to form isopolyanions of various types exhibiting nearly all ratio of V(IV)–V(V) from two V(IV) centers to 18 V(IV) centers [29]. Several types of decavanadium cluster motifs have been previously reported [30–33]. Of the known decavanadium clusters, the decavanadium moiety of VAs-1 is a new type. Another $V_{10}O_{26}$ cluster cage, the isomer of the decanuclear cage of VAs-1, was firstly discovered in the compound $[(C_2H_5)_4N]_4[V_{10}O_{26}]\cdot H_2O$ and reported by a Japanese group later (Fig. 4a) [32,33]. In the former compounds, the decavanadium moiety can be viewed as an octavanadium cluster ring capped with two $V^{IV}O_5$ groups without the encapsulated guest molecule. The distance between the two capping V^{IV} atoms is 4.44 Å. In VAs-1, the decavanadium unit is an octavanadium cube capped with two $V^{V}O_5$ groups (Fig. 4b) with the $V^{V}-V^{V}$ distance of 4.92 Å. The difference between them is the fusing mode with different V^{IV}/V^{V} ratio (Fig. 4).

3.3. Catalytic properties

Vanadium phosphates and vanadium-containing polyoxometalates have shown catalytic activity for selective oxidation in organic synthesis [34–36]. This proved the vanadium species as the active site in the catalysis. Wet catalytic oxidation is an environmentally benign method for fine chemicals. And diphenols including catechol and hydroquinone are important materials in chemical industry. On this view, hydroxylation of phenol using hydrogen peroxide as the oxidant was chosen to investigate the catalytic properties of VAs-1. The results showed that VAs-1 possesses catalytic activity for phenol hydroxylation. Catechol, hydroquinone and benzoquinone are the main products with 15.8% conversion of phenol. The product distribution indicates that hydroquinone prevails with yield of 59.6% at 60°C for 6 h in water. Generally, the catalytic activity and product selectivity in phenol hydroxylation are strongly influenced by solvent, reaction time and temperature, which are investigated as follows.

3.3.1. Influence of solvents

The solvent is known to have profound influence on phenol conversion and the ratio of catechol to hydroquinone. Table 4 presents the catalytic data for phenol hydroxylation over VAs-1 in different solvents at 50°C

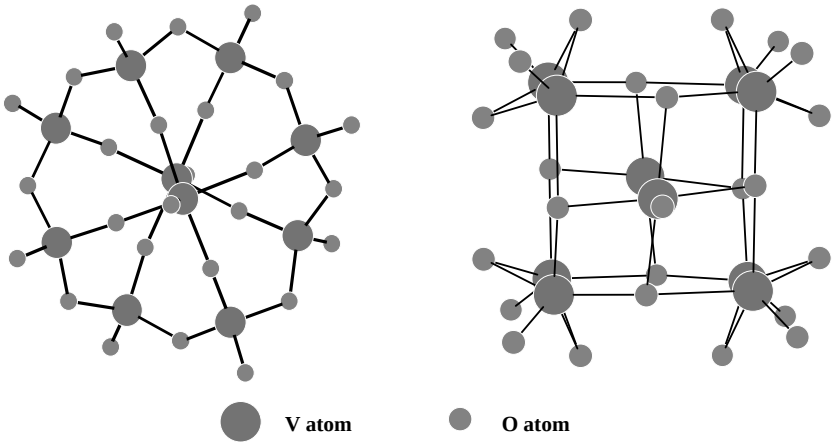

Fig. 4. The two types of decavanadium cluster cages in $[(C_2H_5)_4N]_4[V_{10}O_{26}]\cdot H_2O$ (a) and VAs-1 (b) showing the different fusing modes.

Table 4
Influences of solvents[a]

Solvents	Phenol conversion (%)	Product distribution (%)		
		CAT (%)	HQ (%)	BQ (%)
Water	15.25	38.1	59.9	2.1
Ethyl cyanide	1.90	11.6	88.4	—
Acetone	2.53	—	100.0	—
Methanol	0.27	—	100.0	—
Acetic acid	4.86	4.9	95.1	—
Dichloroethane	8.06	89.4	10.6	—

[a]The reactions were performed in 10 mL solvent at 50°C for 6 h. CAT: catechol; HQ: hydroquinone; BQ: benzoquinone.

Table 5
Influences of reaction time[a]

Reaction time (h)	Phenol conversion (%)	Product distribution		
		CAT (%)	HQ (%)	BQ (%)
1	1.19	—	—	100.0
2	9.14	29.3	61.3	9.0
3	12.92	31.3	64.7	4.0
4	14.07	35.2	62.2	2.6
6	15.84	38.4	59.6	2.0
8	12.88	38.8	59.5	1.8
12	10.36	39.1	59.7	1.2

[a]The reactions were carried out in 10 mL water at 60°C.

for 6 h. When methanol is chosen, almost no reaction takes place. Reaction in dichloroethane gives better result with the phenol conversion of 8.1% and nearly 90% selectivity of catechol. When water is used as the solvent, the reaction shows much higher turnover (15.3%) with high selectivity of hydroquinone. These results indicate that water is most favorable for improving phenol conversion and product selectivity as well. The solvent-induced variation of the catalitic selectivity maybe originates from the different reaction mechanisms. In water, the radical mechanism is possible. The mechanism like that takes place over titanosilicates maybe occurs in organic solvents [37].

3.3.2. Influence of reaction time

Different reaction time has regular influence on phenol hydroxylation. The dependence of catalytic activity on reaction time in water at 60°C is given in Table 5. During the first 6 h, the phenol conversion increases (15.8% at 6 h) with the reaction time prolonged. Then it turns to decline (12.88% at 8 h and 10.36% at 12 h). In the whole process, the yields of benzenquinone declined gradually (from 100.0% at 1 h to 1.2% at 12 h) and the selectivities for catechol and hydroquinone increase. This indicates that low residence time gives rise to low conversion and undesirable product selectivity with high concentration of benzenquinone. It also shows that benzenquinone forms at the first stage. Catechol and hydroquinone form gradually when the reaction time is prolonged. Further prolonging the reaction time will lead to decreasing of the effective phenol conversion due to the deep oxidation. These results clarified that the reaction time should be kept at 6 h.

3.3.3. Influence of reaction temperature

Table 6 shows the influence of reaction temperature on catalytic activity with reaction time setting at 6 h in water. Below 60°C, the conversion of phenol increases with reaction temperature augmented. When the temperature increases over 60°C, the turnover of phenol declines due to the formation of the secondary product

Table 6
Influences of reaction temperature[a]

Temperature (°C)	Phenol conversion (%)	Product distribution (%)		
		CAT (%)	HQ (%)	BQ (%)
40	14.41	41.4	56.3	2.3
50	15.25	38.1	59.9	2.1
60	15.84	38.4	59.6	2.0
70	13.36	39.3	58.8	1.9

[a]The reactions were performed in 10 mL water for 6 h.

of tar. It also indicates that the selectivity of bezenequinone declined with the augmentation of temperature. This suggests that the optimal catalytic reaction temperature is 60°C.

Acknowledgments

We thank the State Key Laboratory of Inorganic Synthesis and Preparative Chemistry, Jilin Universiy for financial support and Prof. Ruji Wang (Tsinghua University) for structural determination.

References

[1] A. Muller, H. Reuter, S. Dillinger, Angew. Chem. Int. Ed. Engl. 34 (1995) 2328.
[2] M. Fujita, K. Umemoto, N. Yoshizawa, N. Fujita, T. Kusukawa, K. Biradha, Chem. Commun. (2001) 509.
[3] J.C. MacDonald, P.C. Dorrestein, M.M. Pilley, M.M. Foote, J.L. Lundburg, R.W. Henning, A.J. Schultz, J.L. Manson, J. Am. Chem. Soc. 122 (2000) 11692.
[4] C.L. Bowes, G.A. Ozin, Adv. Mater. 8 (1996) 13.
[5] A.K. Cheetham, G. Ferey, T. Loiseau, Angew. Chem. Int. Ed. 38 (1999) 3268.
[6] C.N.R. Rao, S. Natarajan, A. Choudhury, S. Neeraj, A.A. Ayi, Acc. Chem. Res. 34 (2001) 80.
[7] J.M. Thomas, R. Raja, Chem. Commun. (2001) 675.
[8] (a) X. Bu, P. Feng, G.D. Stucky, Science 278 (1997) 2080.
(b) P. Feng, X. Bu, G.D. Stucky, Nature 388 (1997) 795.
[9] (a) A.M. Chippindale, A.D. Bond, A.R. Cowley, A.V. Powell, Chem. Mater. 9 (1997) 2830.
(b) A.M. Chippindale, A.R. Cowley, R.I. Walton, J. Mater. Chem. 6 (1996) 611.
[10] (a) T.E. Gier, G.D. Stucky, Nature 349 (1991) 508.
(b) G. Centi, F. Trifire, J.R. Ebner, V.M. Franchett, Chem. Rev. 88 (1988) 55.
(c) G. Albert, Acc. Chem. Res. 11 (1978) 163.
(d) A. Clearfield, Chem. Rev. 88 (1988) 125.
(e) K.H. Lii, Y.F. Huang, V. Zima, C.Y. Huang, H.M. Lin, Y.C. Jiang, F.L. Liao, S.L. Wang, Chem. Mater. 10 (1998) 2609 and references therein.
[11] J. Zubieta, Comments Inorg. Chem. 16 (1994) 153.
[12] V. Soghomonian, R.C. Haushalter, Q. Chen, J. Zubieta, Inorg. Chem. 33 (1994) 1700.
[13] V. Soghomonian, Q. Chen, Y. Zhang, R.C. Haushalter, C.J. O'Connor, C. Tao, J. Zubieta, Inorg. Chem. 34 (1995) 3509.
[14] G. Bonavia, J. Debord, R.C. Haushalter, D. Rose, J. Zubieta, Chem. Mater. 7 (1995) 1995.
[15] D. Riou, F. Taulelle, G. Ferey, Inorg. Chem. 35 (1996) 6392.
[16] M. Roca, M.D. Marcos, P. Amoros, A. Beltran-porter, A.J. Edwards, D. Beltran-porter, Inorg. Chem. 35 (1996) 5613.
[17] Y. Lu, R.C. Haushalter, J. Zubieta, Inorg. Chimica Acta 268 (1998) 257 and references therein.
[18] Z. Bircsak, W.T.A. Harrison, Inorg. Chem. 37 (1998) 3204.
[19] V. Soghomonian, Q. Chen, R.C. Haushalter, J. Zubieta, C.J. O'Connor, Science 259 (1993) 1569.
[20] M.I. Khan, L.M. Meyer, R.C. Haushalter, A.L. Schweitzer, J. Zubieta, J.L. Dye, Chem. Mater. 8 (1996) 43.
[21] V. Soshomanian, Q. Chen, R.C. Haushalter, J. Zubieta, Angew. Chem. Int. Ed. Engl. 32 (1993) 610.
[22] Y. Zhao, G. Zhu, W. Liu, Y. Zou, W. Pang, Chem. Commun. (1999) 2219.
[23] Y. Zhao, Z. Shi, S. Ding, N. Bai, W. Liu, Y. Zou, G. Zhu, P. Zhang, Z. Mai, W. Pang, Chem. Mater. 12 (2000) 2550.
[24] C.J. Warren, R.C. Haushalter, D.J. Rose, J. Zubieta, Inorg. Chem. Commun. 1 (1998) 4.
[25] I.D. Brown, D. Altermatt, Acta Crystallogr. B 41 (1985) 244.
[26] (a) A. Muller, K. Hovemieir, R. Rohlfing, Angew. Chem. Int. Ed. Engl. 31 (1992) 1192.
(b) A. Muller, K. Hovemieir, E. Krickemeyer, H. Bogge, Angew. Chem. Int. Ed. Engl. 33 (1994) 760.
[27] D.D. Hunrich, K. Folting, W.E. Steib, J.C. Huffman, G. Chistou, J. Chem. Soc. Chem. Commun. (1989) 1411.
[28] W.M. Meier, D.H. Olson, Atlas of Zeolite Structure Types, American Chemical Society, Washington, DC, 1989.
[29] M.I. Khan, E. Yohannes, D. Powell, Chem. Commun. (1999) 23.
[30] M.I. Khan, Q. Chen, D.P. Goshorn, H. Hope, S. Parkin, J. Zubieta, J. Am. Chem. Soc. 114 (1992) 3341.
[31] (a) M. Kondo, K. Fujimoto, T. Okubo, A. Asami, S. Noro, S. Kitagawa, T. Ishii, H. Matsuzaka, Chem. Lett. (1999) 291;
(b) S. Nakamura, T. Ozeki, J. Chem. Soc. Dalton Trans. (2001) 472.
[32] A. Bino, S. Cohen, C. Heitner-Wirguin, Inorg. Chem. 21 (1982) 429.
[33] Y. Hayashi, N. Miyakoshi, T. Shinguchi, A. Ueharu, Chem. Lett. (2001) 170.
[34] N.A. Alekar, V. Indira, S.B. Halligudi, D. Srinivas, S. Gopinathan, C. Gopinathan, J. Mol. Catal. A 164 (2000) 181.
[35] K. Nomiya, H. Yanagibayashi, C. Nozaki, K. Kondoh, E. Hiramatsu, Y. Shimizu, J. Mol. Catal. A 114 (1996) 181.
[36] Athilakshmi, B. Viswanathan, React. Kinet. Catal. Lett. 64 (1998) 193.
[37] D.R.C. Huybrechts, L. De Bruycker, P.A. Jacobs, Nature 345 (1990) 240;
R. Murugavel, H.W. Roesky, Angew. Chem. Inter. Ed. Engl. 36 (1997) 477.